International Journal of Robotics and Automation, Vol. 40, No. 10, 2025
An Open Access Paper

JERK-CONTINUOUS ONLINE TRAJECTORY PLANNING AND FEEDFORWARD CONTROL FOR FLEXIBLE JOINT ROBOTS

Pengxiao Jia,* Yifeng Li,* and Jianhua Yang**

Abstract

This paper presents a novel seventh-degree polynomial joint space trajectory planning algorithm. This algorithm features continuous jerk, enabling efficient online computation and handling of singular configurations in robotic systems. Furthermore, a fourth-order feedforward controller is implemented to investigate vibration control in flexible joint robots. Comparative experiments demonstrate the proposed trajectory planning algorithm's ability to generate smoother trajectories. The fourth-order feedforward control effectively leverages information from the reference trajectory. The combined approach of the proposed trajectory planning algorithm and fourth-order feedforward control significantly enhances the control performance of flexible joint robots.

Key Words

Trajectory planning, feedforward control, flexible joint robots, jerk

1. Introduction

Robotics has witnessed widespread adoption across various industries due to their efficiency and safety benefits [1], [2]. In most robotic operations, the end effector must move precisely along a specified trajectory. Therefore, trajectory planning is an important element in robotics research [3], [4]. In the process of trajectory planning, the first step is to plan a series of waypoints within the Cartesian space. These Cartesian waypoints are then transformed into joint space waypoints through inverse kinematics. Finally, joint space trajectory planning is performed on the joint space waypoints, so that the Cartesian motion is ultimately converted into the motion of individual joints. However, when the robot is in a singular configuration, the inverse Jacobian matrix does not exist, making it impossible to calculate the velocity and acceleration in the joint space. Therefore, a joint space trajectory planning method that can handle the robot's singular configurations is required. This method should ensure continuous position, velocity, and acceleration at all waypoints to guarantee smooth and stable motion of the robot's end effector. Furthermore, online computational efficiency is essential for non-technical applications [5].

Beyond accurate trajectory tracking, robotic speed is critical for maximising productivity in many applications. There has been a significant amount of research on time-optimal trajectory planning for robots [6]–[9]. However, traditional approaches often involve abrupt acceleration changes, which can excite structural resonance and lead to severe robot vibrations [10], [11]. This issue is further compounded by the growing trend of lightweight robotics, utilising flexible materials and structures [12]. To mitigate these challenges, smooth, jerk-bounded trajectories are highly desirable. Such trajectories minimise vibration excitation, ultimately enhancing tracking performance and positional accuracy throughout the motion [13]. Polynomial-based approaches have emerged as the dominant method for generating smooth, jerk-limited trajectories, offering a balance of smoothness, dynamic performance, and computational efficiency [14]. In [15], a new method to enhance the payload capacity of robotic manipulators by optimising cubic spline and Bernstein polynomial trajectories is proposed. In [16], a time-optimal trajectory planning method based on quintic Pythagorean-hodograph (PH) curves is proposed to realise the smooth and stable high-speed operation of the Delta parallel robot. Nevertheless, these methods do not ensure the continuity of the jerk along the entire trajectory. As demonstrated in [17], the undesirable jerk impulse occurring at the start and end points can have an adverse impact on positioning accuracy. To further mitigate the adverse effects of jerk and achieve even higher levels of continuity and regularity in the motion profiles, some research has explored the use of higher-order polynomial functions for trajectory generation.

* College of Science, Beijing Forestry University, Beijing, 100083, China; e-mail: pxaij@bjfu.edu.cn; 2463095569@qq.com
** Research Institute of Wood Industry, Chinese Academy of Forestry, Beijing 100091, China; e-mail: woodtesting@163.com
Corresponding author: Jianhua Yang

Recommended by Dan Zhang
(DOI: 10.2316/J.2025.206-1208)

Feedforward control strategies utilise detailed trajectory information, such as polynomial coefficients or spline parameters, to calculate precise control signals. This approach is frequently paired with trajectory planning to enhance the performance of motion control systems. In [18], an algorithm for calculating higher-order trajectories with bounds on all considered derivatives for point-to-point moves of electromechanical motion systems is proposed by using fourth-order feedforward with fourth-order trajectories. In [19], a feedforward control technique that employs cycloid functions, taking polynomial functions as inputs, to generate trajectories for point-to-point motion with suppressed residual vibrations is proposed.

Motivated by the above work, the principal objective of this research is to propose a seventh-degree polynomial joint space trajectory planning algorithm with continuous jerk, designed for efficient online computation and capable of handling singular configurations in robotic systems. Additionally, in conjunction with this algorithm, a fourth-order feedforward controller is employed to investigate vibration control in flexible joint robots, thereby enhancing the overall performance and precision of motion control in such systems. The main contributions of this paper are as follows.

(1) A novel online trajectory planning algorithm is proposed by using seventh-degree polynomials to satisfy the continuity of joint's jerk as well as the controllability of the jerk at the end path point to avoid system vibration and ensure the stability of robot motion. Besides, the algorithm can be used when the robot is in singular configurations.
(2) In conjunction with this algorithm, a fourth-order feedforward controller is employed to investigate vibration control in flexible joint robots. Feedforward control can better exploit the smooth information of the trajectory, thereby achieving superior control performance.

The paper is organised as follows. In Section 2, the jerk-continuous online trajectory planning algorithm in joint space is presented in detail. The fourth-order feedforward control for flexible systems is introduced in Section 3. In Section 4, the effectiveness of combining the fourth-order feedforward control with the trajectory planning algorithm proposed in this paper is verified through comparative simulation and experimental results. The summary of the results obtained is given in Section 5.

2. Jerk-Continuous Online Trajectory Planning

To illustrate our proposed trajectory planning algorithm, we analyse an example taken from [5]. As shown in Fig. 1, there are three segments which are determined by the four waypoints in joint space. The waypoints in joint space are obtained via inverse kinematics from the waypoints in Cartesian space. Let q, $\dot{q}$, $\ddot{q}$, and $\dddot{q}$ represent the position, velocity, acceleration, and jerk in joint space, respectively. T_i represents the interval between the ith waypoint and the $(i+1)$th waypoint. T_i is equal to zero when the ith waypoint is the terminal one. *INVALID* represents the joint velocity or acceleration at singular configurations.

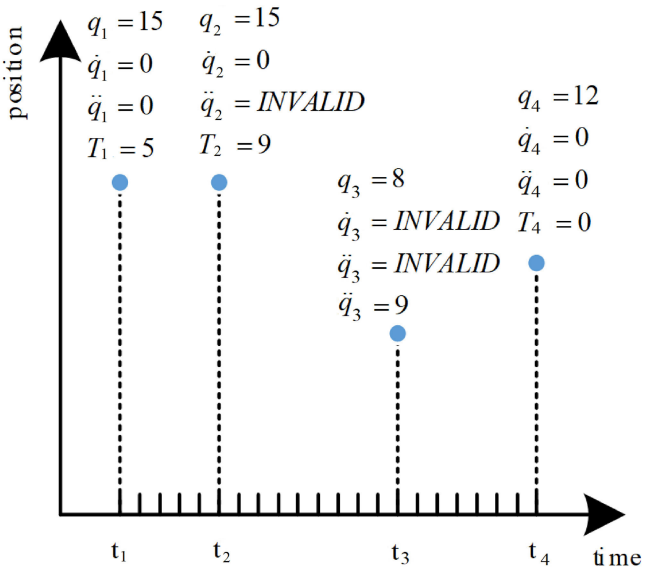

Figure 1. The waypoints in joint space.

First, we define a normalised time variable u. u starts at 1 at the beginning of each trajectory segment and decreases to 0 at the endpoint.

$$u = 1 - \frac{t - t_{i-1}}{t_i - t_{i-1}} = 1 - \frac{t - t_{i-1}}{T_i} \tag{1}$$

The proposed planning algorithm proceeds by grouping two or three joint space waypoints together for trajectory planning. In this algorithm, the position and velocity at the start and end points of the trajectory segments are given. Depending on whether the velocities at the second and third points are known or unknown, the algorithm addresses three distinct cases.

Case I: If the second point is not in a singular configuration, with q_2, $\dot{q}_2$, $\ddot{q}_2$, and $\dddot{q}_2$ are all known, the trajectory between the first and second points is described using a seventh-degree polynomial:

$$\begin{aligned} p(u) = {} & c_7u^7 + c_6u^6 + c_5u^5 + c_4u^4 + c_3u^3 \\ & + c_2u^2 + c_1u + c_0 \end{aligned} \tag{2}$$

The known boundary conditions are listed as:

$$\begin{cases} p(1) = q_1 \\ p(0) = q_2 \\ \dot{p}(1) = \dot{q}_1 \\ \dot{p}(0) = \dot{q}_2 \\ \ddot{p}(1) = \ddot{q}_1 \\ \ddot{p}(0) = \ddot{q}_2 \\ \dddot{p}(1) = \dddot{q}_1 \\ \dddot{p}(0) = \dddot{q}_2 \end{cases} \tag{3}$$

Solving (3) yields:

$$\begin{aligned} c_7 = {} & -20q_1 + 20q_2 - 10T_1\dot{q}_1 - 10T_1\dot{q}_2 - 2\ddot{q}_1T_1^2 \\ & + 2\ddot{q}_2T_1^2 - 0.1667\dddot{q}_1T_1^3 - 0.1667\dddot{q}_2T_1^3 \end{aligned}$$

$$
\begin{aligned}
c_6 &= 70q_1 - 70q_2 + 34T_1\dot{q}_1 + 36T_1\dot{q}_2 + 6.5\dddot{q}_1T_1^2 \\
&\quad -7.5\dddot{q}_2T_1^2 + 0.5\ddddot{q}_1T_1^3 + 0.6667\ddddot{q}_2T_1^3 \\
c_5 &= -84q_1 + 84q_2 - 39T_1\dot{q}_1 - 45T_1\dot{q}_2 - 7\dddot{q}_1T_1^2 \\
&\quad +10\dddot{q}_2T_1^2 - 0.5\ddddot{q}_1T_1^3 - \ddddot{q}_2T_1^3 \\
c_4 &= 35q_1 - 35q_2 + 15T_1\dot{q}_1 + 20T_1\dot{q}_2 + 2.5\dddot{q}_1T_1^2 \\
&\quad -5\dddot{q}_2T_1^2 + 0.1667\ddddot{q}_1T_1^3 + 0.6667\ddddot{q}_2T_1^3 \\
c_3 &= -0.1667\ddddot{q}_2T_1^3 \\
c_2 &= 0.5\dddot{q}_2T_1^2 \\
c_1 &= -T_1\dot{q}_2 \\
c_0 &= q_2
\end{aligned} \tag{4}
$$

Case II: If the second point is at a singular configuration while the third point is not, then the trajectory between the first and second points can be described by a sixth-degree polynomial, whereas the trajectory between the second and third points can be described by a quintic polynomial.

$$
\begin{aligned}
p_1(u) &= c_{61}u^6 + c_{51}u^5 + c_{41}u^4 + c_{31}u^3 \\
&\quad +c_{21}u^2 + c_{11}u + c_{01} \qquad (5) \\
p_2(u) &= c_{52}u^5 + c_{42}u^4 + c_{32}u^3 \\
&\quad +c_{22}u^2 + c_{12}u + c_{02} \qquad (6)
\end{aligned}
$$

The known boundary conditions are listed as:

$$
\begin{cases}
p_1(1) = q_1 \\
p_1(0) = q_2 \\
p_2(1) = q_2 \\
p_2(0) = q_3 \\
\dot{p}_1(1) = \dot{q}_1 \\
\ddot{p}_1(1) = \ddot{q}_1 \\
\dddot{p}_1(1) = \dddot{q}_1
\end{cases} \tag{7}
$$

The two segments of trajectories meet at the second point with continuous velocity, acceleration, and jerk.

Solving (7) yields:

$$
\begin{aligned}
c_{61} &= \frac{\begin{pmatrix} -28\dot{q}_1T_1 + 28\dot{q}_3T_1 - 8\ddot{q}_1T_1^2 - 8\ddot{q}_3T_1^2 - \dddot{q}_1T_1^3 \\ +\dddot{q}_3T_1^3 - 40q_1 + 80q_2 - 40q_3 \end{pmatrix}}{8} \\
c_{51} &= \frac{\begin{pmatrix} 2172\dot{q}_1T_1 - 2460\dot{q}_3T_1 + 588\ddot{q}_1T_1^2 + 708\ddot{q}_3T_1^2 \\ +65\dddot{q}_1T_1^3 - 89\dddot{q}_3T_1^3 \\ +3192q_1 - 6672q_2 + 3480q_3 \end{pmatrix}}{192} \\
c_{41} &= \frac{\begin{pmatrix} -540\dot{q}_1T_1 + 780\dot{q}_3T_1 - 132\ddot{q}_1T_1^2 - 228\ddot{q}_3T_1^2 \\ -13\dddot{q}_1T_1^3 + 29\dddot{q}_3T_1^3 \\ -840q_1 + 1920q_2 - 1080q_3 \end{pmatrix}}{48} \\
c_{31} &= \frac{\begin{pmatrix} 60\dot{q}_1T_1 - 220\dot{q}_3T_1 + 12\ddot{q}_1T_1^2 + 68\ddot{q}_3T_1^2 \\ +\dddot{q}_1T_1^3 - 9\dddot{q}_3T_1^3 + 120q_1 \\ -400q_2 + 280q_3 \end{pmatrix}}{32} \\
c_{21} &= \frac{\begin{pmatrix} 60\dot{q}_1T_1 - 60\dot{q}_3T_1 + 12\ddot{q}_1T_1^2 + 12\ddot{q}_3T_1^2 \\ +\dddot{q}_1T_1^3 - \dddot{q}_3T_1^3 + 120q_1 - 240q_2 + 120q_3 \end{pmatrix}}{48} \\
c_{11} &= \frac{\begin{pmatrix} 60\dot{q}_1T_1 + 228\dot{q}_3T_1 + 12\ddot{q}_1T_1^2 - 60\ddot{q}_3T_1^2 \\ +\dddot{q}_1T_1^3 + 7\dddot{q}_3T_1^3 + 120q_1 + 240q_2 - 360q_3 \end{pmatrix}}{192} \\
c_{01} &= q_2
\end{aligned} \tag{8}
$$

Case III: If both the second and third points are at singular configurations, then the trajectory between the first and second points can be described by a quintic polynomial, while the trajectory between the second and third points can be represented by a cubic polynomial.

$$
\begin{aligned}
p_1(u) &= c_{51}u^5 + c_{41}u^4 + c_{31}u^3 + c_{21}u^2 \\
&\quad +c_{11}u + c_{01} \qquad (9) \\
p_2(u) &= c_{32}u^3 + c_{22}u^2 + c_{12}u + c_{02} \qquad (10)
\end{aligned}
$$

The known boundary conditions are listed as:

$$
\begin{cases}
p_1(1) = q_1 \\
p_1(0) = q_2 \\
p_2(1) = q_2 \\
p_2(0) = q_3 \\
\dot{p}_1(1) = \dot{q}_1 \\
\ddot{p}_1(1) = \ddot{q}_1 \\
\dddot{p}_1(1) = \dddot{q}_1
\end{cases} \tag{11}
$$

The two segments of trajectories meet at the second point with continuous velocity, acceleration, and jerk.

Solving (11) yields:

$$
\begin{aligned}
c_{51} &= \frac{(-78\dot{q}_1T_1 - 33\ddot{q}_1T_1^2 - 7\dddot{q}_1T_1^3 - 84q_1 + 90q_2 - 6q_3)}{66} \\
c_{41} &= \frac{(246\dot{q}_1T_1 + 99\ddot{q}_1T_1^2 + 17\dddot{q}_1T_1^3 + 270q_1 - 294q_2 + 24q_3)}{66} \\
c_{31} &= \frac{(-68\dot{q}_1T_1 - 22\ddot{q}_1T_1^2 - 3\dddot{q}_1T_1^3 - 80q_1 + 92q_2 - 12q_3)}{22} \\
c_{21} &= \frac{(-84\dot{q}_1T_1 - 33\ddot{q}_1T_1^2 - 5\dddot{q}_1T_1^3 - 60q_1 + 36q_2 + 24q_3)}{66} \\
c_{11} &= \frac{(120\dot{q}_1T_1 + 33\ddot{q}_1T_1^2 + 4\dddot{q}_1T_1^3 + 180q_1 - 174q_2 - 6q_3)}{66} \\
c_{01} &= q_2
\end{aligned} \tag{12}
$$

Up to this point, the velocities, accelerations, and jerks for all joint path points have been determined, ensuring that the generated joint space trajectory has continuous position, velocity, acceleration, and jerk profiles.

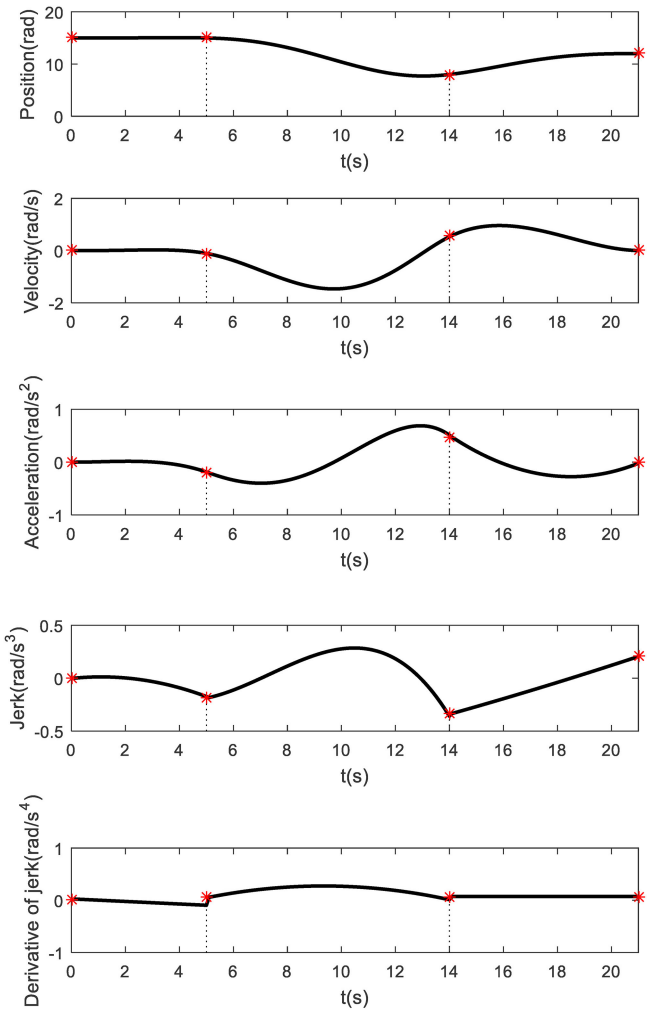

Figure 2. The trajectory planning results for data from Fig. 1.

Figure 2 illustrates the planned trajectory resulting from the trajectory planning algorithm proposed in this paper. All the waypoints' data information is derived from Fig. 1. From Fig. 2, we can see that the position curve, the velocity curve, and the acceleration curve are all smooth and continuous. The trajectory planning algorithm proposed can ensure the continuity of jerk and the acceleration at the start and end points are controller to zero in order to avoid the system vibration and ensure the smooth movement of the robot.

3. Fourth-Order Feedforward Control

In the control of rigid models, feedforward control is commonly employed, such as velocity feedforward and acceleration feedforward. This section, inspired by the control approach for flexible motor axles presented in [20], analyses the fourth-order feedforward control for a two-mass spring system with flexibility.

As shown in Fig. 3, it depicts a two-mass spring model. J_1denotes the inertia of the actuator, J_2 the inertia of the load, τ_m the torque supplied by the actuating device, θ_1 the actuator position, θ_2 the load position, k the stiffness

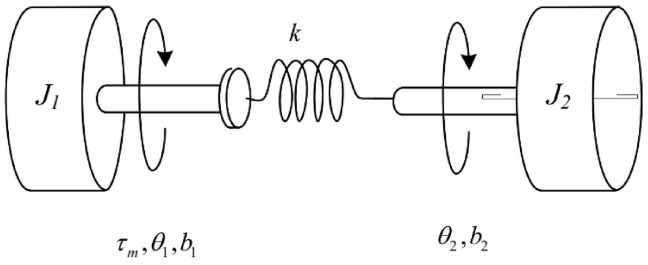

Figure 3. Two-mass spring system.

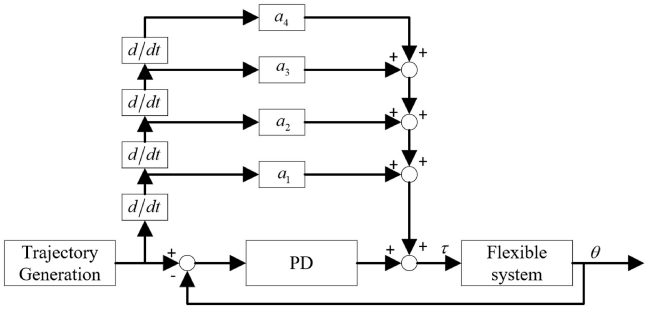

Figure 4. Fourth-order feedforward implementation.

between the masses, and b_1 and b_2, respectively, represent the damping coefficients during the rotation of the two masses. The equations of motion for this flexible system are:

$$\begin{aligned} J_1\ddot{\theta}_1 + b_1\dot{\theta}_1 + k(\theta_1 - \theta_2) &= \tau_m \\ J_2\ddot{\theta}_2 + b_2\dot{\theta}_2 - k(\theta_1 - \theta_2) &= 0 \end{aligned} \tag{13}$$

Performing the Laplace transform on (13) yields the following transfer function:

$$\tau_m = \frac{a_4 s^4 + a_3 s^3 + a_2 s^2 + a_1 s}{k}\theta_2 \tag{14}$$

with:

$$\begin{aligned} a_4 &= J_1 J_2 \\ a_3 &= J_1 b_1 + J_2 b_2 \\ a_2 &= (J_1 + J_2)k + b_1 b_2 \\ a_1 &= (b_1 + b_2)k \end{aligned} \tag{15}$$

This implies that if the fourth derivative of the trajectory θ_2 exists, that is, the velocity, acceleration, jerk, and the derivative of jerk exist, the fourth-order feedforward control law can be calculated as:

$$\tau_m = \frac{1}{k}(a_4 \dddot{\theta}_2 + a_3 \dddot{\theta}_2 + a_2\ddot{\theta}_2 + a_1\dot{\theta}_2) \tag{16}$$

This feedforward control scheme can be conveniently implemented, as shown in Fig. 4, where "Flexible system" represents the flexible joint robot.

4. Simulation and Experimental Results

To validate the effectiveness of combining the fourth-order feedforward control with the trajectory planning

algorithm proposed in this paper, numerical simulation and real experiment are performed in this section. First, the numerical simulation results are given, and then the experimental device with flexible joint has been designed and the real experimental results are presented.

4.1 Simulation Results

Consider the single-link flexible-joint manipulator described in [21]. Assuming that the link is rigid and ignoring the viscous damping, its dynamic equations are expressed as follows:

$$\begin{aligned} D\ddot{q}_l + mgl\sin(q_l) + k(q_l - q_r) &= 0 \\ J\ddot{q}_r - k(q_l - q_r) &= \tau \end{aligned} \tag{17}$$

where $q_l \in R$ denotes the link position, $q_r \in R$ denotes the motor position, D is the link inertia, J is the motor inertia, m is the link mass, k is the stiffness, l is the centre of mass, g is the gravity constant, and τ is the control torque. The parameters are consistent with those in [21].

Consider the joint space trajectory of the flexible joint manipulator comprises nine path points, the ith path point is denoted as $P_i : [q_i, \dot{q}_i, \ddot{q}_i, \dddot{q}_i, T_i]$.

$$\begin{aligned} P_1 &: [0.0000, 0.0000, 0.0000, 0.0000, 0.5] \\ P_2 &: [0.0041, 0.0327, 0.1963, 0.7850, 0.5] \\ P_3 &: [0.0573, 0.1963, 0.3927, 0.0000, 0.5] \\ P_4 &: [0.2004, 0.3600, 0.1963, -0.7854, 0.5] \\ P_5 &: [0.3927, 0.3927, 0.0000, 0.0000, 0.5] \\ P_6 &: [0.5850, 0.3600, -0.1963, -0.7854, 0.5] \\ P_7 &: [0.7281, 0.1963, -0.3927, 0.0000, 0.5] \\ P_8 &: [0.7813, 0.0327, -0.1963, 0.7854, 0.5] \\ P_9 &: [0.7854, 0.0000, 0.0000, 0.0000, 0.5] \end{aligned}$$

For comparative simulation, the commonly used position–velocity–time (PVT) trajectory planning algorithm in motion controller is adopted as a comparison [22].

Figure 5 illustrates the joint space trajectories planned by both the PVT trajectory planning algorithm and the jerk-continuous trajectory planning algorithm proposed in this paper, based on nine joint path points, P_1–P_9. As can be seen from Fig. 5, both trajectory planning algorithms, when based on the same set of path points, yield trajectories with position and velocity profiles that are essentially identical. The PVT trajectory planning algorithm utilises only the position and velocity information of the joint path points to complete the planning process. This algorithm ensures continuity in position and velocity, but results in discontinuities in jerk, with the derivative of jerk being non-existent. The jerk-continuous trajectory planning algorithm proposed in this paper employs position, velocity, acceleration, and jerk information for trajectory planning. This algorithm ensures the continuity of jerk, with the derivative of jerk being well defined, resulting in smoother trajectories compared to those generated by the PVT algorithm.

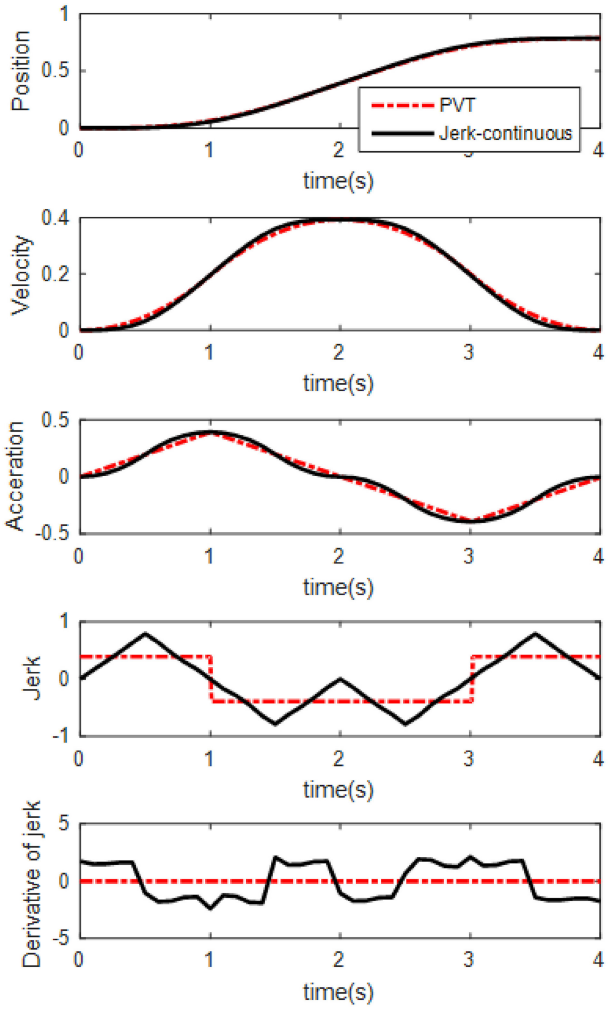

Figure 5. Comparison between the two trajectory planning algorithms.

To validate the effectiveness of the proposed jerk-continuous trajectory planning algorithm combined with fourth-order feedforward control in vibration control of flexible joint robot, the following two comparative experiments were conducted. The first experiment adopts the proposed jerk-continuous trajectory planning algorithm combined with fourth-order feedforward control, the control scheme depicted in Fig. 4, and the feedback control is implemented using a PID controller. In the second experiment, a PID controller with identical parameters is utilised, however, the trajectory planning is carried out using the PVT algorithm, and no feedforward control is employed. The comparative experimental results are illustrated in Figs. 6 and 7.

As can be seen from the figures, the fourth-order feedforward controller effectively leverages the information embedded in the smoother reference trajectory provided by the proposed jerk-continuous planning method. The combination of this jerk-continuous trajectory planning approach with the fourth-order feedforward control significantly enhances the control performance of the flexible-joint robot, leading to a substantial suppression of residual vibrations after the flexible joint reaches a steady state.

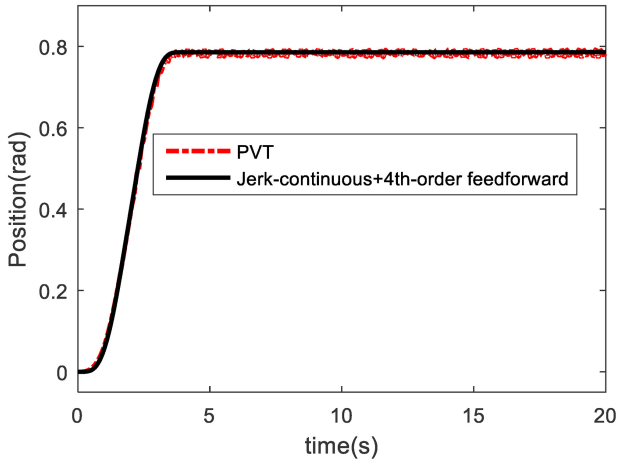

Figure 6. Position control of two comparative experiments.

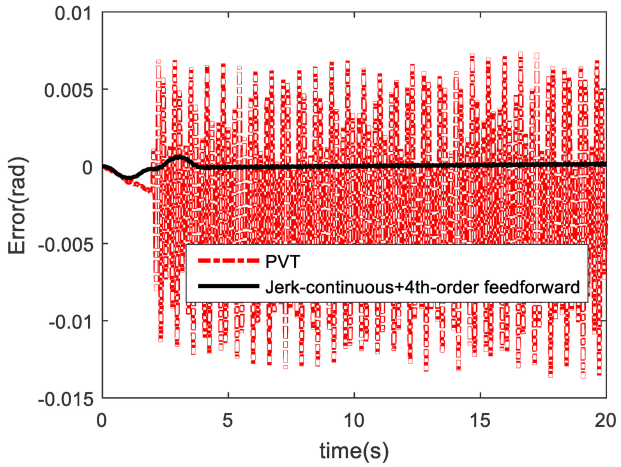

Figure 7. Position errors of two comparative experiments.

4.2 Experimental Results

To validate the effectiveness of the proposed jerk-continuous trajectory planning algorithm combined with fourth-order feedforward control in practical situations, an experimental device with flexible joint has been designed and real experimental results are presented.

4.2.1 Experimental Setup

To conduct experimental research, we designed a single-joint robotic arm experiment platform with flexible joint (harmonic gear) as shown in Fig. 8. The experimental platform mainly consists of the robotic arm itself and a controller. The robotic arm is composed of a link, a harmonic reducer, a coupling, a servo motor, and a base. The reducer used is a harmonic gear reducer with a reduction ratio of 1:80 (model XB1-50-80). The servo motor is a Yaskawa AC servo motor, model SGMPH01A1A6C. The controller is composed of a self-developed DSP motion controller and a servo driver. An accelerometer (model 3DM-GX1) is installed at the end of the robotic arm to detect vibration signals. The servo motor drives the link through the harmonic reducer to achieve rotational

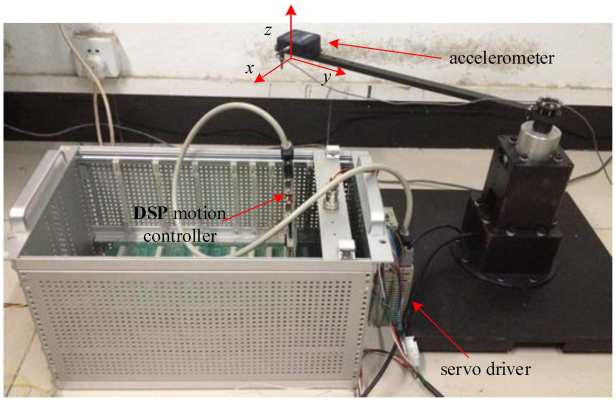

Figure 8. Experimental system.

movement in the horizontal plane. The installation direction of the accelerometer is as shown in Fig. 8, with the X-axis oriented tangentially to the rotational movement of the link. Since the link rotates within the horizontal plane, by measuring the acceleration in the X-axis direction, the amplitude of the vibration can be determined.

4.2.2 Experimental Comparison

The servo cycle of the DSP motion controller is set to 0.5 ms. To verify the effectiveness of the method proposed in this paper, the trapezoidal move profile is used for comparison. The acceleration time is 0.01 s, the constant speed time is 0.8 s, and the deceleration time is 0.01 s. The acceleration during the acceleration phase is 20,000 rad/s^2, and the acceleration during the deceleration phase is -20,000 rad/s^2. The operating time of the robotic arm is 0.82 s, and the motion of the link after 0.82 s is considered residual vibration, with the starting moment of residual vibration at 0.82 s. Experimental results indicate that the cutoff time for noticeable residual vibration is 2 s. The jerk-continuous trajectory is designed using the method proposed in Section 2, with $c_7 = 3240$, $c_6 = -11340$, $c_5 = 13608$, $c_4 = -5670$, $c_3 = 0$, $c_2 = 0$, $c_1 = 0$, and $c_0 = 162$. Since it is difficult to establish an accurate model of the real system and the model parameters are time-varying, the parameters in the fourth-order feedforward controller are determined using a trial-and-error method, with $a_4 = 10^{-4}$, $a_3 = 0$, $a_2 = 0.1$, and $a_1 = 0$. Due to the residual vibration occurring after 0.82 s, only the acceleration changes after 0.82 s are analysed, as shown in Fig. 9. As shown in Fig. 9, when the reference trajectory is the trapezoidal move profile, the robotic arm exhibits significant residual vibration, demonstrating that the harmonic reducer has a certain degree of flexibility, which leads to residual vibrations in the robotic arm due to joint flexibility. When the jerk-continuous trajectory proposed in this paper is used in conjunction with the fourth-order feedforward control, the amplitude of the residual vibration is greatly reduced, indicating that the proposed method can effectively suppress residual vibrations caused by joint flexibility. Moreover, the method presented in this paper does not require changes to the existing control structure of the flexible joint robotic

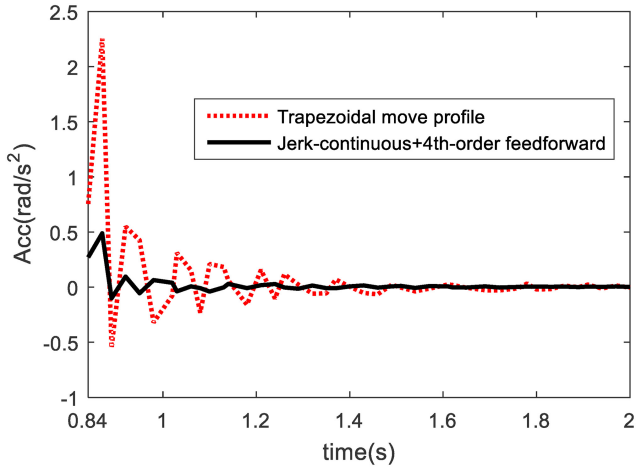

Figure 9. Experimental results.

arm, nor does it necessitate additional sensors, making it easier to implement in practical engineering applications and demonstrating clear advantages over other control methods. Nevertheless, from the point of view of control accuracy, if the sensors can be used to collect information, such as the angle and angular velocity of the link, there are already many excellent nonlinear control algorithms and intelligent control algorithms that can achieve better control results. Therefore, we will next continue to study the improvement of the accuracy of vibration control for flexible joint robots without changing the robot structure or adding sensors as much as possible.

5. Conclusion

This paper proposes a novel trajectory planning algorithm in robot joint space. Additionally, in conjunction with this algorithm, a fourth-order feedforward controller is employed to investigate vibration control in flexible joint robots. The proposed trajectory planning algorithm poses several good properties: first, it provides the continuity of jerk on all segments of the planning trajectory, second, it can handle singular configurations in robotic systems, and third, it can be applied to online planning by looking ahead one or two waypoints. The fourth-order feedforward control more effectively utilises the information from the reference trajectory. Combining the trajectory planning algorithm proposed with fourth-order feedforward control proves to be efficacious in enhancing the control performance of flexible joint robots.

References

[1] Y. Fang, J. Qi, J. Hu, W. Wang, and Y. Peng, An approach for jerk-continuous trajectory generation of robotic manipulators with kinematical constraints, *Mechanism and Machine Theory*, *153*, 2020, 103957.

[2] M. Moghaddam and S.Y. Nof, Parallelism of pick-and-place operations by multi-gripper robotic arms, *Robotics and Computer-Integrated Manufacturing*, *42*, 2016, 135–146.

[3] J. Ogbemhe, K. Mpofu, and N. Tlale, Optimal trajectory scheme for robotic welding along complex joints using a hybrid multi-objective genetic algorithm, *IEEE Access*, *7*, 2019, 158753–158769.

[4] J.Z. Zhao, S.Z. Wang, A.B. Jiang, J. Xiao, and B. Wang, Trajectory planning of 6-DOF manipulator based on Gaussian process regression method, *International Journal of Robotics and Automation*, *35*(3), 2020, 209–220.

[5] F. Jing, Y. Qi, Y. Qiang, and C. Yang, An on-line robot trajectory planning algorithm in joint space with continuous accelerations, in *Proceeding International Conf. on Advanced Technology of Design and Manufacture (ATDM 2010)*, Beijing, 2010, 372–377.

[6] E.S. Moghaddam, M.G. Saryazd, and A. Taghvaeipour, Trajectory optimization of a spot-welding robot in the joint and Cartesian spaces, *International Journal of Robotics and Automation*, *38*(2), 2023, 109–125.

[7] C.Y. Li, Y.S. Chao, S. Chen, J.R. Li, and Y. P. Yuan, Time-optimal trajectory generation for industrial robots based on elite mutation sparrow search algorithm, *International Journal of Robotics and Automation*, *38*(2), 2023, 126–135.

[8] Z.Y. He, X.J. Tang, Q. Shen, C.X. Duan, and C.F. Jia, Optimisation of a six-degree-of-freedom robot trajectory based on improved multi-objective PSO algorithm, *International Journal of Robotics and Automation*, *38*(3), 2023, 218–230.

[9] S.P. Zhao, Z.X. Zhu, C.B. Chen, Y.S. Du, X.H. Song, K. Yan, D.C. Jiang, L. Li, and A. Liu, Optimisation of a six-degree-of-freedom robot trajectory based on improved multi-objective PSO algorithm, *International Journal of Robotics and Automation*, *38*(5), 2023, 344–351.

[10] H. Heo, Y. Son, and J. Kim, A trapezoidal velocity profile generator for position control using a feedback strategy, *Energies*, *12*(7), 2019, 1222.

[11] D. Thomsen, R. Knudsen, D. Brandt, O. Balling, and X. Zhang, Generating vibration free rest-to-rest trajectories for configuration dependent dynamic systems via 3-segmented input shaping, in *Proceeding IEEE International Conf. on Robotics and Automation (ICRA)*, Brisbane, QLD, 2018, 4361–4366.

[12] M. Korayem and S. Dehkordi, Dynamic modeling of flexible cooperative mobile manipulator with revolute-prismatic joints for the purpose of moving common object with closed kinematic chain using the recursive Gibbs–Appell formulation, *Mechanism and Machine Theory*, *137*, 2019, 254–279.

[13] T. Zhang, M. Zhang, and Y. Zou, Time-optimal and smooth trajectory planning for robot manipulators, *International Journal of Control, Automation and Systems*, *19*(1), 2021, 521–531.

[14] M. Arsenault, L. Tremblay, and M. Zeinali, Optimization of trajectory durations based on flow rate scaling for a 4-DoF semi-automated hydraulic rockreaker, *Mechanism and Machine Theory*, *143*, 2020, 103632.

[15] A. Gallant and C. Gosselin, Extending the capabilities of robotic manipulators using trajectory optimization, *Mechanism and Machine Theory*, 121, 2018, 502–514.

[16] T. Su, L. Cheng, Y. Wang, X. Liang, J. Zheng, and H. Zhang, Time-optimal trajectory planning for delta robot based on quintic Pythagorean-hodograph curves, *IEEE Access*, 6, 2018, 28530–28539.

[17] A. Visioli, Trajectory planning of robot manipulators by using algebraic and trigonometric splines, *Robotica*, *18*(6), 2000,.611–631.

[18] M. Huang, Y. Hsu, and R. Fung, Minimum-energy point-to-point trajectory planning for a motor-toggle servomechanism, *IEEE/ASME Transactions on Mechatronics*, *17*(2), 2011,337–344.

[19] A. Abe and K. Hashimoto, A novel feedforward control technique for a flexible dual manipulator, *Robotics and Computer-Integrated Manufacturing*, *35*, 2015,169–177.

[20] P. Lambrechts, M. Boerlage, and M. Steinbuch, Trajectory planning and feedforward design for electromechanical motion systems, *Control Engineering Practice*, *13*(2), 2005, 145–157.

[21] P. Jia, Design of a novel NNs learning tracking controller for robotic manipulator with joints flexibility, *Journal of Robotics*, *2023*, 2023, 1186719.

[22] G.C. Wang, *Research on Forward Control Algorithm of Six Degree of Freedom Series Manipulator*, Doctoral Dissertation, Shandong University, Shandong, China, 2020.

Biographies

Pengxiao Jia received the Ph.D. degree from the Institute of Automation, Chinese Academy of Science, Beijing, China, in 2014. He is currently an Associate Professor with the College of Science, Beijing Forestry University. His research interests include neural networks, nonlinear control, and robot control.

Yifeng Li is currently pursuing the bachelors degree in electronic information science and technology with Beijing Forestry University. His current research interests include adaptive backstepping control, nonlinear system control, and robot control.

Jianhua Yang is currently a Researcher with the Research Institute of Wood Industry, Chinese Academy of Forestry. His research interests include artificial intelligence and forestry equipment and informatisation.